

## Microwave absorbing properties of $\text{La}_{0.8}\text{Ba}_{0.2}\text{MnO}_3$ nano-particles

ZHOU Ke-sheng(周克省), DENG Jian-jie(邓建杰), YIN Li-song(尹荔松),  
MA Shi-hong(马诗宏), GAO Song-hua(高松华)

School of Physics Science and Technology, Central South University, Changsha 410083, China

Received 8 January 2007; accepted 8 May 2007

**Abstract:**  $\text{La}_{0.8}\text{Ba}_{0.2}\text{MnO}_3$  nano-particles were synthesized by sol-gel process, and the crystal structure and morphology were characterized by XRD and SEM, respectively. The complex permittivity and permeability were determined by microwave vector network analyzer in the frequency range of 2–18 GHz. The relationship between reflection coefficient and microwave frequency of  $\text{La}_{0.8}\text{Ba}_{0.2}\text{MnO}_3$  was calculated based on measured data. The results show that the average diameter of  $\text{La}_{0.8}\text{Ba}_{0.2}\text{MnO}_3$  crystal powders is about 80 nm and the crystal structure is perovskite when being calcined at 800 °C for 2 h. The microwave absorbing peak is 13 dB at 6.7 GHz and the effective absorbing bandwidth above 10 dB reaches 1.8 GHz for the sample with the thickness of 2.6 mm. The microwave absorption can be attributed to both the dielectric loss and the magnetic loss from the loss tangents of the sample, but the former is greater than the latter.

**Key words:**  $\text{La}_{0.8}\text{Ba}_{0.2}\text{MnO}_3$ ; nano-particles; microwave absorbing materials; electromagnetic loss; sol-gel

### 1 Introduction

Microwave absorbing materials have an important application in the military and the civil technology such as the stealth, microwave darkroom and electromagnetic interference protection[1]. People have been attracted by  $\text{La}_{1-x}\text{T}_x\text{MnO}_3$  (T=Sr, Ca, Ba) for many years because of its special electromagnetism characteristic, especially colossal magnetoresistance effect[2–7], which was widely reported. In addition, the colossal magnetoresistance of  $\text{LaMnO}_3$  doped by Te, Ce, Zr or Sn at site A and other element at site B was studied[8–11]. The doped rare-earth oxide can exhibit rich electromagnetism characteristics such as magnetic transformation and conductivity change, which provides a foundation for the electromagnetic wave absorbing materials in the theory and the experiment. In Ref.[12], the microwave absorbing properties of  $\text{Ba}_{1-x}\text{La}_x\text{Zn}_x\text{Fe}_{12-x-y}(\text{Me}_{0.5}\text{Mn}_{0.5})_y\text{O}_{19}$  (Me=Zr, Sn) in frequency range of 1–20 GHz were studied and the absorption was as high as 40 dB when the thickness of sample was less than 1 mm, however, the disadvantage was that the effective bandwidth is very narrow (smaller than 1 GHz). Refs.[13–14] reported that  $\text{La}_{1-x}\text{Sr}_x\text{MnO}_3$  prepared by

solid state reaction method had excellent property, the microwave absorbing bandwidth above 8 dB was 3 GHz and the peak was 25 dB when  $x=0.5$  in the frequency range of 8–12 GHz, but the frequency spectra characteristic of complex permittivity and permeability was not studied carefully. In Ref.[15], the microwave absorbing property of  $\text{La}_{1-x}\text{Sr}_x\text{Mn}_{1-y}\text{Fe}_y\text{O}_3$  powders prepared by sol-gel method was studied in the frequency range of 2–18 GHz, which is better than that of  $\text{La}_{1-x}\text{Sr}_x\text{MnO}_3$  in microwave absorbing bandwidth and intensity.

The study on electromagnetic response mechanism of  $\text{LaMnO}_3$  that is doped at site A by other element such as Ba is a worthy topic of microwave absorbing materials in both the theory and the application, but there are not such reports so far. In this study, nanometer  $\text{La}_{0.8}\text{Ba}_{0.2}\text{MnO}_3$  powders were prepared with sol-gel process and their microwave absorption properties and physical mechanism were discussed in the frequency range of 2–18 GHz.

### 2 Experimental

The sol-gel process was used to prepare  $\text{La}_{0.8}\text{Ba}_{0.2}\text{MnO}_3$  nano-particles. High purity compounds

of  $\text{La}_2\text{O}_3$ ,  $\text{Mn}(\text{C}_2\text{H}_4\text{O}_2)_2$ ,  $\text{Ba}(\text{OH})_2$  powders were weighed according to the mole fraction (2:5:1) and dissolved in dilute nitric acid, respectively. Then the above solutions were slowly put into the EDTA solution, mixed fully together at  $70^\circ\text{C}$ , reacted for 6 h and evaporated in oven so that the white powders were obtained. The powders were changed into the black  $\text{La}_{0.8}\text{Ba}_{0.2}\text{MnO}_3$  samples after being calcined at  $800^\circ\text{C}$  for 2 h.

The crystal structure of the sample was determined by X-ray diffraction (XRD) with a D/max-III A of Japan,  $\text{CuK}_\alpha$  radiation and the voltage/current of 35 kV/25 mA. The morphology and size of powder particles of the sample were observed by a scanning electron microscopy (SEM) (JSM-5600 LV).

The prepared powders of  $\text{La}_{0.8}\text{Ba}_{0.2}\text{MnO}_3$  were mixed with paraffin wax according to mass ratio of 7:3 and pressed into annular sample with 2.6 mm in thickness. The complex permittivity and permeability of the sample were measured by HP8722ES microwave vector network analyzer in the frequency range of 2–18 GHz.

### 3 Results and discussion

#### 3.1 Structure and morphology of sample

Fig.1 shows the X-ray diffraction pattern of  $\text{La}_{0.8}\text{Ba}_{0.2}\text{MnO}_3$ . From Fig.1, all peaks are attributed to cubic perovskite structure. Fig.2 shows the SEM photograph of  $\text{La}_{0.8}\text{Ba}_{0.2}\text{MnO}_3$  crystalline powders with irregular spherical shape and an average diameter about 80 nm.

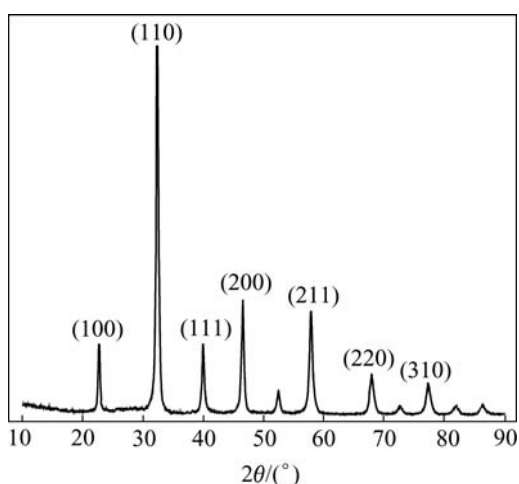


Fig.1 XRD pattern of  $\text{La}_{0.8}\text{Ba}_{0.2}\text{MnO}_3$

#### 3.2 Microwave electromagnetic spectra of sample

Fig.3 shows the permittivity spectra of  $\text{La}_{0.8}\text{Ba}_{0.2}\text{MnO}_3$ . The real part ( $\epsilon'$ ) of the permittivity decreases with the increase of frequency from 2 GHz to 18 GHz. The imaginary part ( $\epsilon''$ ) of the permittivity first

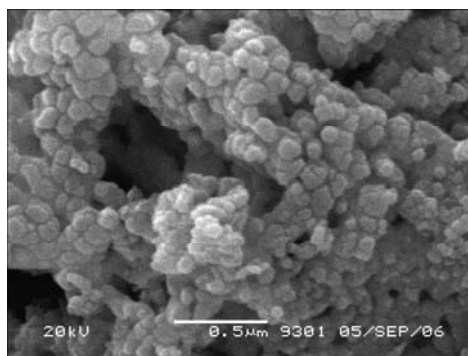


Fig.2 SEM image of  $\text{La}_{0.8}\text{Ba}_{0.2}\text{MnO}_3$  crystalline powders

increases and then decreases, which shows a peak at 5.2 GHz. Fig.4 shows the permeability spectra of  $\text{La}_{0.8}\text{Ba}_{0.2}\text{MnO}_3$ . The real part ( $\mu'$ ) of the permeability first decreases and then increases with the increase of frequency, but this change is slight. The imaginary part ( $\mu''$ ) of the permeability first increases and then decreases slightly, which has a smaller peak at about 14.8 GHz. By comparing Fig.3 with Fig.4, it can be found that the maximum value of the imaginary part ( $\epsilon''$ ) of the permittivity is 11 that appears in low frequency position,

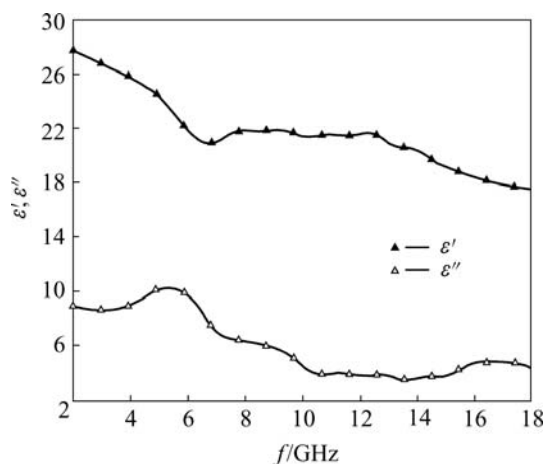


Fig.3 Permittivity of  $\text{La}_{0.8}\text{Ba}_{0.2}\text{MnO}_3$  at different frequency

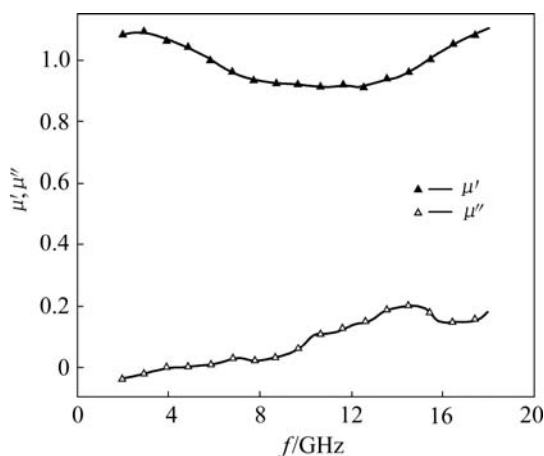


Fig.4 Permeability of  $\text{La}_{0.8}\text{Ba}_{0.2}\text{MnO}_3$  at different frequency

but the maximum value of the imaginary part ( $\mu''$ ) of the permeability is 0.2 that appears in high frequency position.

### 3.3 Microwave absorbing properties of sample

According to the equations of Ref.[16], the relation between the reflectance( $R$ ) of  $\text{La}_{0.8}\text{Ba}_{0.2}\text{MnO}_3$  and frequency( $f$ ) can be calculated from measured data of the permeability and permittivity. The equations are as follows:

$$Z_{in} = \sqrt{\mu_r / \varepsilon_r} \tanh[j(2\pi d/\lambda)\sqrt{\varepsilon_r \mu_r}]$$

$$R = 20 \lg |(Z_{in} - 1)/(Z_{in} + 1)|$$

where  $Z_{in}$  is the normalized input impedance when the electromagnetic wave incidences vertically to the specimen.  $\varepsilon_r$  is the complex permittivity ( $\varepsilon_r = \varepsilon' - j\varepsilon''$ ).  $\mu_r$  is the complex permeability ( $\mu_r = \mu' - j\mu''$ ).  $\lambda$  is the wavelength.  $d$  is the thickness of the sample. Fig.5 shows the relation between the reflectance( $R$ ) of  $\text{La}_{0.8}\text{Ba}_{0.2}\text{MnO}_3$  and the microwave frequency( $f$ ) in range of 2–18 GHz when the thickness of sample is 2.6 mm.  $R$  decreases fast from 2 GHz to 6.7 GHz, then increases from 6.7 GHz to 13 GHz and decreases from 13 GHz to 18 GHz. This indicates that  $\text{La}_{0.8}\text{Ba}_{0.2}\text{MnO}_3$  has certain microwave absorbing properties in the frequency range of 2–18 GHz, whose value of the absorbing peak is 13 dB at 6.7 GHz and the absorbing bandwidth above 10 dB is 1.8 GHz.

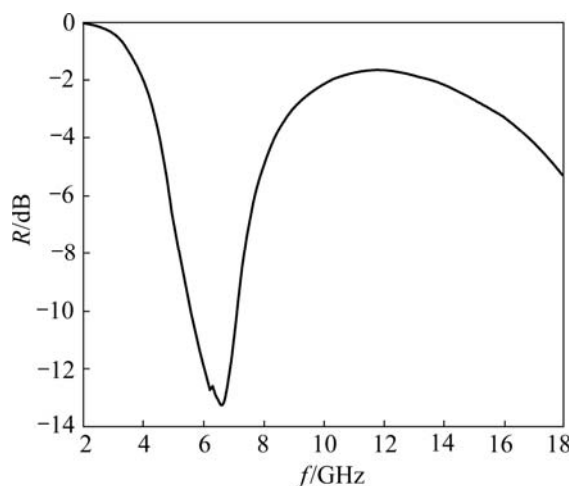


Fig.5 Relationship between reflectance and microwave frequency for  $\text{La}_{0.8}\text{Ba}_{0.2}\text{MnO}_3$

### 3.4 Microwave loss mechanism of sample

The dielectric and magnetic loss tangents in the frequency range of 2–18 GHz are shown in Fig.6. It can be discovered that the dielectric loss tangent ( $\tan\delta_e$ ) is much larger than the magnetic loss tangent ( $\tan\delta_m$ ) in low frequency band, but they are close in high frequency

band. The result shows that the dielectric loss is main in low frequency band, and both the dielectric and magnetic loss affect together in high frequency band. Therefore, the reflectivity peak in Fig.5 at 6.7 GHz is mainly caused by dielectric loss. There are maximum values of  $\tan\delta_e$  and  $\tan\delta_m$  respectively above 13 GHz (Fig.6), so the microwave absorption from 13 GHz to 18 GHz may be caused by both dielectric and magnetic losses, which brings about decline of the reflectance (Fig.5).

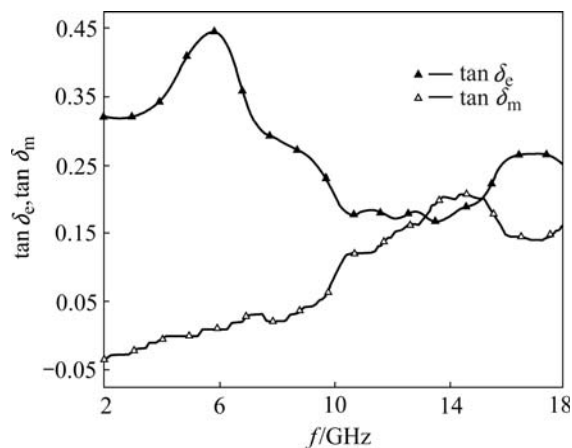


Fig.6 Relationships between  $\tan\delta_e$  or  $\tan\delta_m$  and microwave frequency for  $\text{La}_{0.8}\text{Ba}_{0.2}\text{MnO}_3$

The anti-ferromagnetic structure of  $\text{LaMnO}_3$  can result in dielectric loss without doping, and it changes into ferromagnetic structure that can result in magnetic loss when doped by  $\text{Ba}^{2+}$ . The  $\text{Mn}^{4+}$  appears and the crystal structure changes from low symmetry to high one, so that there are two transitions from insulator state to conductor or semiconductor and from anti-ferromagnetic state to ferromagnetic[17], which can be explained by double exchange theory[18].

So  $\text{La}_{0.8}\text{Ba}_{0.2}\text{MnO}_3$  nano-particles have certain magnetism and magnetic loss in microwave field, but the dielectric loss is still predominant. There are both dielectric and magnetic losses for  $\text{La}_{0.8}\text{Ba}_{0.2}\text{MnO}_3$ . In addition, there are atomic clusters such as anti-ferromagnetic and ferromagnetic clusters in the sample, which have different magnetism and compete with each other[19]. The  $\tan\delta_m$  exhibits rising tendency and the  $\tan\delta_e$  exists decreasing tendency with the increase of microwave frequency. The reason is that anti-ferromagnetic clusters transform into ferromagnetic clusters constantly by absorbing electromagnetic energy in microwave field.

## 4 Conclusions

1)  $\text{La}_{0.8}\text{Ba}_{0.2}\text{MnO}_3$  nano-particles have microwave absorbing properties both in low and high frequency band in range of 2–18 GHz. The value of microwave

absorption in low frequency band is larger than that in high frequency, the bandwidth above 10 dB is 1.8 GHz, and the peak of reflection coefficient is 13 dB at the frequency of 6.7 GHz. Such materials exhibit good microwave absorbing properties. The system of  $\text{La}_{0.8}\text{Ba}_{0.2}\text{MnO}_3$  doped at site B or compounded with other materials can have better microwave absorption in bandwidth and intensity because of modulating electromagnetic parameters by doping or cooperation effects.

2)  $\text{La}_{0.8}\text{Ba}_{0.2}\text{MnO}_3$  nano-particles exhibit certain magnetic properties because of being doped by  $\text{Ba}^{2+}$  at site A and have both dielectric and magnetic losses under the microwave field, but the dielectric loss is more important and the magneticless mainly appears in high frequency band.

## References

- [1] BARTON D K. Radar evaluation handbook [M]. New York: Artech House, 1998.
- [2] LIU J M, WANG K F. Colossal magnetoresistive manganites [J]. Progress in Physics, 2005, 25(1): 82–130.
- [3] HU F X, GAO J, WU X S. Controllable colossal electroresistance in  $\text{La}_{0.8}\text{Ca}_{0.2}\text{MnO}_3$  epitaxial thin films [J]. Physical Review B, 2005, 72(064428): 1–5.
- [4] OKUYUMA S, TAKENAKA K, SHIOZAKI R, SAWAKI Y, SUGAI S. Optical reflectivity study on magnetoresistive manganese perovskites: impurity effect on the ferromagnetic-metallic and charge-ordered states [J]. Physica B, 2003, 329/333: 846–847.
- [5] DAI D S, XIONG G C, WU S C. Structure, electromagnetic properties and colossal magneto-resistance of  $\text{Re}_{1-x}\text{T}_x\text{MnO}_3$  [J]. Progress in Physics, 1997, 17: 201–221.
- [6] TOMOHIKO N, YUTAKA U. Structures and electromagnetic properties of the A-site disordered Ba-based manganites:  $\text{R}_{0.5}\text{Ba}_{0.5}\text{MnO}_3$  (R=Y and rare earth elements) [J]. Journal of Alloys and Compounds, 2004, 383: 135–139.
- [7] NAM Y S, JU H L, PARK C W. Low field magnetoresistance in intrinsic granular system  $\text{La}_{1-x}\text{Ba}_x\text{MnO}_3$  [J]. Solid State Communications, 2001, 119: 613–618.
- [8] CHOU H, WU C B, HSU S G, WU C Y. Electron-doped magnetoresistance in the sintered  $\text{La}_{1-x}\text{T}_x\text{MnO}_3$  lanthanum-deficient phase [J]. Physical Review B, 2006, 74(17): 44051–44057.
- [9] GAVATHRI N, RAVCHAUDHURI A, TIWARY S. Electrical transport, magnetism, and magnetoresistance in ferromagnetic oxides with mixed exchange interactions: A study of the  $\text{La}_{0.7}\text{Ca}_{0.3}\text{Mn}_{1-x}\text{Co}_x\text{O}_3$  system [J]. Phys Rev B, 1997, 56(3): 1345–1353.
- [10] YUAN X B, LIU Y H, HUANG B X, WANG C J, ZHANG R Z, MEI L M. Enhancement of low field magnetoresistance in Bi-doped  $\text{La}_{0.67}\text{Ba}_{0.33}\text{MnO}_3$  [J]. Journal of the Chinese Rare Earth Society, 2004, 22(3): 336–340.
- [11] TAKASHI O, ADARSH S, MASAFUMI C, HIROMASA T, YOSHIHARU K. Electrical and magnetic properties of  $\text{La}_{1-x}\text{Bi}_x\text{MnO}_3$  [J]. Journal of Magnetism and Magnetic Materials, 2005, 290/291: 933–936.
- [12] KAGOTANI T, FUJIWARA D, SUGIMOTO S, INOMATA K, HOMMA M. Enhancement of GHz electromagnetic wave absorption characteristics in aligned M-type barium ferrite  $\text{Ba}_{1-x}\text{La}_x\text{Zn}_x\text{Fe}_{12-x-y}(\text{Me}_{0.5}\text{Mn}_{0.5})_y\text{O}_{19}$  ( $x=0.00-0.5$ ;  $y=1.0-3.0$ ,  $\text{Me}=\text{Zr, Sn}$ ) by metal substitution [J]. Journal of Magnetism and Magnetic Materials, 2004, 272/276: e1813–e18155.
- [13] LI G, HU G G, ZHOU G H. Attractive microwave-absorbing properties of  $\text{La}_{1-x}\text{Sr}_x\text{MnO}_3$  manganite powders [J]. Materials Chemistry and Physics, 2002, 75: 101–104.
- [14] HU G G, YIN P, LÜ Q R. Attractive microwave-absorbing properties and conduct of  $\text{LaSr}_{1-x}\text{MnO}_3$  [J]. Journal of the Chinese Rare Earth Society, 2002, 20(2): 179–181.
- [15] ZHOU Ke-sheng, WANG Da, YIN Li-song, KONG De-ming, HUANG Ke-long. Electromagnetic properties and loss mechanism of  $\text{LaSr}_{1-x}\text{MnO}_3$  in microwave band [J]. The Chinese Journal of Nonferrous Metals, 2006, 16(5): 753–757. (in Chinese)
- [16] WU X G, CHE Y Q. International microwave absorption material [M]. Changsha: National University of Defense Technology Press, 1992. (in Chinese)
- [17] DUN P, TAN G T, DAI S Y, CHEN Z H, ZHOU Y L, LÜ H B. Colossal magnetoresistance effect in the perovskite-type  $\text{La}_{0.9}\text{Sb}_{0.1}\text{MnO}_3$  material [J]. Acta Physica Sinica, 2003, 52(08): 2061–2064.
- [18] ZENER C. Interaction between the *d*-Shells in the transition metals (II): Ferromagnetic compounds of manganese with perovskite structure [J]. Phys Rev, 1950, 82(3): 403–405.
- [19] HU J F, MEI L M, DING Z Q, FU G, ZHAO W J, ZHANG Q Q, LIU Y H. Magnetoresistance effects in  $\text{La}_{0.65}(\text{Ca, Ba})_{0.35}\text{Mn}_{1-x}\text{Fe}_x\text{O}_y$  [J]. Chinese Rare Earths, 2000, 21(1): 19–22.

(Edited by HE Xue-feng)